BROOKHAVEN
NATIONAL LABORATORY

BNL-79556-2007-CP

Polarization Studies of CdZnTe Detectors using Synchrotron X-ray Radiation

G. S. Camarda, A. E. Bolotnikov, *Member, IEEE*, , Y. Cui, *Member, IEEE*, A. Hossain, and R. B. James, *Fellow, IEEE*

2007 Nuclear Science Symposium, Medical Imaging Conference
Honolulu, Hawaii, October 28th – November 3rd, 2007

Nonproliferation and National Security Department
Detector Development and Testing Division

Brookhaven National Laboratory
P.O. Box 5000
Upton, NY 11973-5000
www.bnl.gov

DISCLAIMER

Polarization Studies of CdZnTe Detectors using Synchrotron X-ray Radiation

G. S. Camarda, A. E. Bolotnikov, *Member, IEEE,* , Y. Cui, *Member, IEEE,* A. Hossain, S. A. Awadalla, J. Mackenzie, and H. Chen, *Member, IEEE,* and R. B. James, *Fellow, IEEE*

Abstract– **High densities of impurities and defects lead to severe charge-carrier trapping that can be major issues in assuring the high performance of CZT detectors. For some medical- imaging applications, the typical X-ray flux can be very high. Under such high irradiation conditions, the trapped charge builds up inside the detector affecting its stability. This phenomenon generally is termed the polarization effect. We conducted detailed studies on polarization in CZT crystals employing a highly collimated synchrotron x-ray radiation source available at Brookhaven's National Synchrotron Light Source (NSLS). We were able to induce polarization effects by irradiating specific areas within the detector. These measurements allowed us to make, for the first time, a quantitative comparison between areas where polarization is induced, and the electron- and hole-collection X-ray maps obtained at low flux, where no polarization is induced. We discuss the results of these polarization studies.**

I. Introduction

CZT is a wide bandgap compound semiconductor that is attractive for room-temperature radiation detectors due to its high sensitivity to gamma rays. However, high densities of impurities and defects in the material can lead to severe charge-carrier trapping that is a major issue in assuring the detectors' high performance. . Single-polarity charge-sensing devices, such as coplanar grid-, virtual Frisch grid-, or pixellated-detectors, offer an effective approach to overcoming hole trapping.. Thus, better than 1% energy resolution at 662 keV was achieved with large volume CZT detectors, making it feasible to use them for many spectroscopic- and low-flux-applications.

Manuscript received November 15, 2007. This work was supported by U.S. Department of Energy, Office of Nonproliferation Research and Engineering, NA-22. The manuscript has been authored by Brookhaven Science Associates, LLC under Contract No. DE-AC02-98CH1-886 with the U.S. Department of Energy.

G. S. Camarda, A. E. Bolotnikov, A. Hossain, Y. Cui, and R. B. James are with Brookhaven National Laboratory, Upton, NY 11793 USA (phone: 631-344-2008; e-mail: giuseppec@bnl.gov).

H. Chen, S. Awadalla, J. Mackenzie are with Redlen Technologies, Sidney, BC V8L 5Y8 Canada (phone: 250-656-5411 x. 242; email: henry.chen@redlen.com).

Grain boundaries and twins degrade the performance of a device, and hence, a first step in screening the CZT crystals is to ensure that they are free of these macroscopic defects. Customarily, we use White beam X-ray diffraction topography (WXDT) measurements at the high-energy NSLS beamline along with IR microscopy to identify the distribution of defects and strains in the bulk of CZT crystals.

A high-intensity X-ray beam collimated down to a 10-micrometer spot size, available at the NSLS, was employed for X-ray mapping to measure the correlation between microscopic defects (inclusions) and variations in the collected charges. Using synchrotron radiation, we earlier demonstrated that single Te inclusions trap a significant amount of the charge of an electron cloud. Te inclusions and their surrounding areas were measured, and the deleterious effects of Te inclusions on the energy spectrum were recorded [1-4].

For some medical-imaging applications, the typical X-ray flux may be very high. Under such high irradiation, the trapped charge builds up inside the detector, and affects its stability. In other words, radiation induces a polarization effect. In this work we explored CZT detectors wherein we induce polarization by using the high flux of the synchrotron radiation, and tentatively offer explanations of the cause of the polarization.

Polarization may depend on several factors including the detector's bias voltage, the X-ray flux, and temperature. Polarization can be partly controlled by adjusting these parameters, such as by increasing bias voltage, lowering the flux, and/or increasing the temperature. .

We assessed the performance and temporal response of some CZT samples from different vendors with our setup at beamline X27B of the NSLS, under varying levels of irradiation. We were able to induce a polarization effect in certain regions of some detectors. The results of these polarization studies are reported here.

II. Experimental Techniques

To understand the factors limiting the performance of CZT detectors and explore the uniformity of their responses, we characterized the devices using the X-ray beam available at National Synchrotron Light Source (NSLS) at Brookhaven National Laboratory (BNL).

To do this, we developed a dedicated testing end-station that at the NSLS's beamline X27B. Significant variations in energy resolution have been observed even for adjacent pixels of the same detector using these radiation-sources. Hence, a special microprobe arrangement is necessary in attempting to correlate the fluctuation in collected charge with the microscopic defects and impurities present in the CZT crystal. Therefore, we chose to use Synchrotron Radiation (SR), a highly collimated high-intensity X-ray beam, undertaking micron-scale performance mapping to measure fluctuations in the collected charge of the CZT detectors; this beam supported measurements of areas as small as 10x10 μm^2, and allowed us to see fluctuations in collected charge over the entire area of the detector in a reasonable time, as low as 0.5 seconds per area interrogated (that is 100 μm^2) and with unique spatial resolution.

Further, we employed X-ray Diffraction Topography (XDT) to assess the degree of perfection of the CZT crystals, These two techniques are detailed in the following paragraphs.

A. Micro-scale Detector Mapping

In clarifying the factors limiting the energy resolution of CZT detectors, we developed an end-station for testing the detectors at the NLSL's beamline X27B. Since these defects are highly localized, simple flood illumination is unsatisfactory.

A microprobe arrangement is needed, in combination with some way to visualize the defects in registration with the electronic tests. We found that infrared (IR) imaging of the raw material is a powerful tool, revealing the tellurium inclusions very easily (seemingly they are the bulk of the defects in our material), and in three dimensions, using confocal techniques. It is impractical to employ radioactive sources to generate a microbeam of radiation with which to probe a detector's electronic performance because its intensity after strict collimation is too low, and hence, testing takes far too long. The NSLS's beamlines generate very bright, highly collimated x-ray beams covering a wide energy range; accordingly, we constructed an apparatus that could be installed in such a beamline for our detailed investigation of a detector's performance. The set up (Fig.1) consists of a fine collimating slit producing a 10μm x 10μm beam, a precision motor-controlled X-Y-Z translation stage on which we mounted a circuit board, the low-noise signal processing system, and the CZT detector perpendicular to the incident beam.

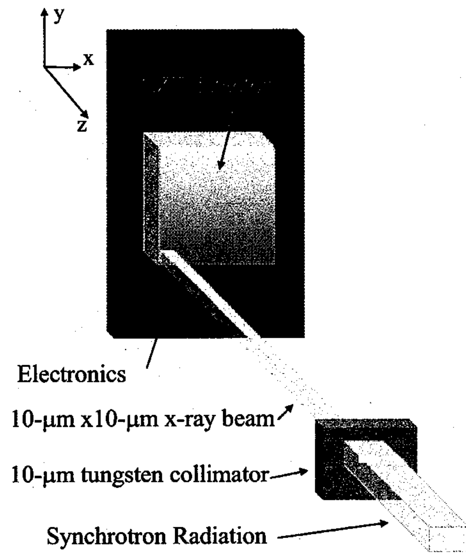

Fig. 1. Set-up for the micro-scale mapping of a CZT detector.

An X-Y raster scan of the detector area is acquired. The energy of the radiation source can be set anywhere between 7- and 40-keV. The system is automatically controlled using SPEC [5], a UNIX-based software package widely used in X-ray diffraction experiments for instrument control and data acquisition, so allowing us to determine, for each area interrogated, the energy spectrum and all the associated information in it, i.e., pulse height, photopeak position, and the FWHM. The high brightness of the source facilitated the acquisition of good statistics in seconds; accordingly, a raster scan of a 3x7 mm^2 CZT detector area was obtained within a few hours. Fig.2a is an example of an X-ray map we obtained, wherein the light grey regions correspond to areas of the detector where collection efficiency is better than that in the vicinity dark grey areas (Fig 2b); Figs c and d, respectively, show the corresponding energy spectra taken in those areas.

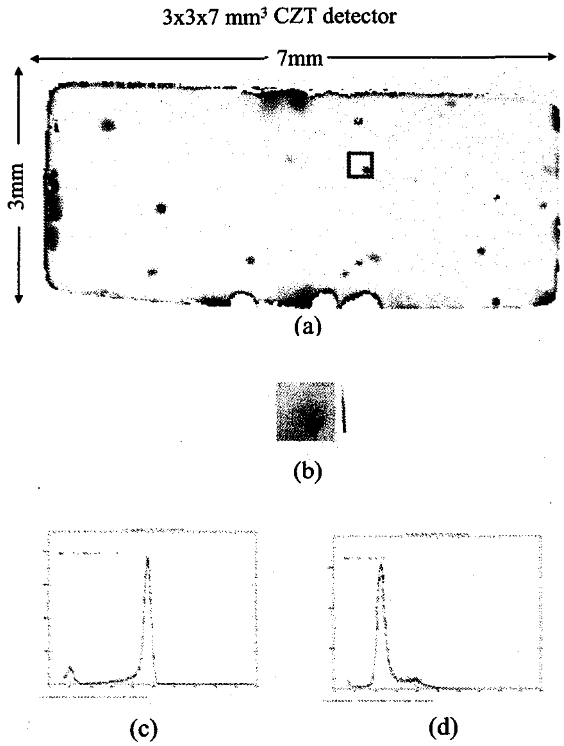

Fig. 2. (a) An x-ray map of a 7x3x3 mm³ CZT detector; (b) X-ray map of a 200μmx200μm area that surrounds a Te inclusion; (c) energy spectrum of a region of the detector where the efficiency of collection is good ; (d) energy spectrum of a region of the detector where it is poor.

B. *X-ray Diffraction Topography*

X-ray topography is not configured for studying surfaces. The topography we are exploring is that of the crystal's diffracting planes, not exterior features; when using this technique to observe dislocations, we are looking at the configuration of the lattice planes around the defects. We accomplished this objective by recording the intensity of the X-rays diffracted from the deformed lattice planes that differ from the intensity diffracted by a perfect crystal, thus forming a localized image of the defect. Essentially, we are using diffraction to probe the crystal's internal structure. However, diffraction is not a point probe, and interpreting the observed contrast is far from a trivial task.

At the simplest level, we can obtain some insight into how the dislocations are imaged in the following way. We consider a perfect crystal that diffracts monochromatic X-ray radiation of wavelength λ from a set of lattice planes spaced d. For a strongly diffracted beam to emerge at an angle $2\theta_B$ to the incident beam, the well-know Bragg relation applies. That is,

$$\lambda=2d\sin\theta_B$$

Clearly, when the orientation of the lattice spacing plane varies locally, e.g., around a dislocation, this relation will not apply simultaneously to the perfect and distorted regions with their differing sets of lattice planes. Consequently, there is a difference in intensity corresponding to the two regions, i.e., an image of the defect.

C. *White X-ray Diffraction Topography (WXDT)*

If a white beam is employed, rather than a monochromatic beam, then the diffracted beams from each point of the crystal can be observed, with different diffractions at different solid angles around the crystal. The Bragg law is applied simultaneously to each point of the crystal to denote the correct x-ray wavelength. The information gathered from this measurement reveals the number of domains and their distribution in the crystal. By adequately preparing a sample and by using high resolution films, single defects might be studied.

White X-ray Diffraction Topography (WXDT) measurements at the beamline X17B1 were taken to investigate more systematically the origins of the crystal mosaicity that can supply information about the distribution of defects and strains in bulk CZT crystals.

Fig.3 shows the setup we employed for this experiment. The crystal is scanned across the 22mm x 0.2mm x-ray beam set by x-y slits. The information is recorded on a 20x25cm imaging plate with a resolution of 50μm. Only a few orders of diffractions will be recorded.

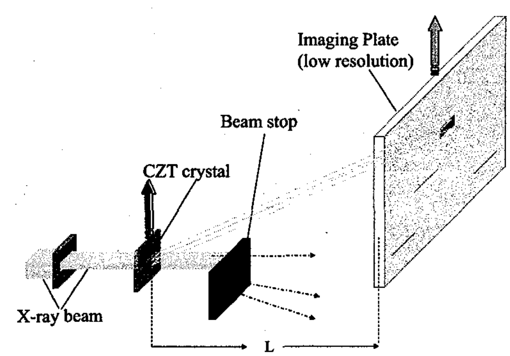

Fig. 3. Set up.for obtaining WXDT measurements from a crystal. The distance L between imaging plate and CZT crystal is 153 cm The imaging plate is scanned in the same direction at the same speed as that of the crystal as it is scanned across the beam.

By using special photographic films a resolution of few micrometers can be achieved. The imaging plate is scanned in the same direction at the same speed as that of the crystal as it is scanned across the beam. Fig. 4 shows the topography of a 27mm x 27mm CZT sample, in which several domains are distinguishable. Each domain encompasses information about single Te inclusions, but better resolution is needed to distinguish between them. In this measurement, the white beam used ranged from 50keV to 200keV. The high flux of the SR allowed us to work in the transmission (Laue) mode, with CZT crystals that were several millimeters thick..

Scanning the CZT crystals is very rapid ; the measurements are completed in a few seconds. Hence, batches

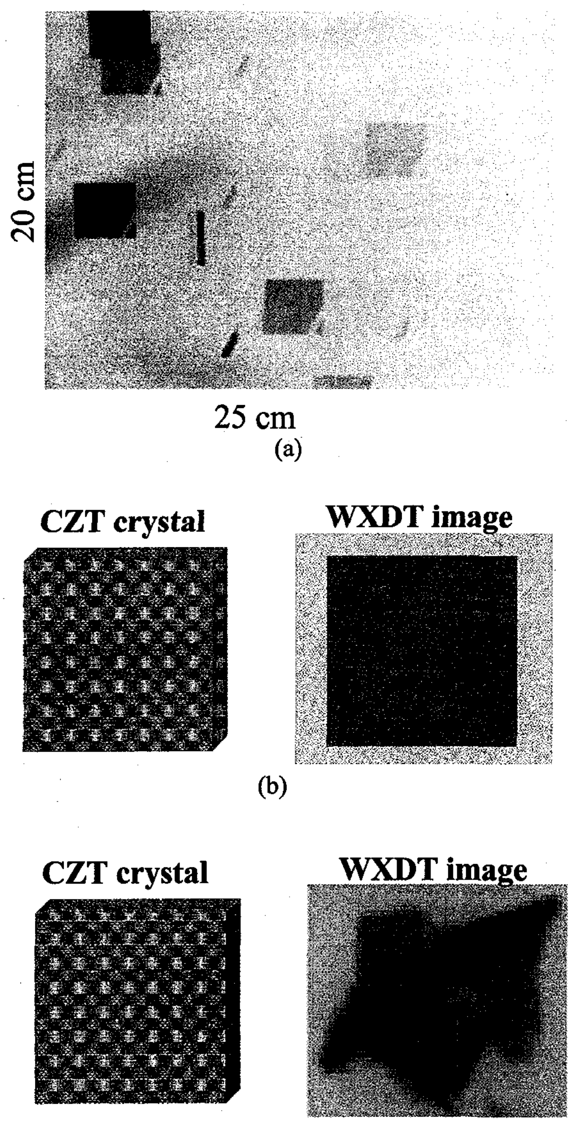

Fig. 4. (a) WXDT image of a 27x27x2mm^3 CZT crystal. This crystal presents three domains and it is possible to distinguish the three different diffracted images. (b)Perfect crystal; the intensity diffracted by the perfect lattice is only one. (c) Imperfect crystal: there is a difference in intensity corresponding to the deformed lattice.

of CZT crystals can be screened quickly. We used this methodology to ensure that the CZT samples are all single crystals.

III. Electron trapping by Te inclusions

Two effects are associated with the Te inclusions. Firstly, they reduce the total amount of the collected charge as the electron cloud drifts towards the anode, in a way similar to that of traps associated with point defects. The total amount of the lost charge is proportional to the drift distance traveled by the electron cloud, and can be described by an exponential decay function with a charge attenuation length, λ. Secondly, because the inclusions trap many electrons per interaction with electron clouds, they cause large fluctuations in the collected charge.

The electron cloud generated by the incident photons is known to become much larger than the size of the typical inclusion after drifting for the first 10 ns [6, 7]. For this reason, defects near the cathode side reveal a better contrast than defects near the anode side, which are blurry.

Thus, the charge trapped by a Te inclusion depends on its effective diameter and its location with respect to the center of the electron cloud.

The output signals are given by the amount of the collected charge. The reduction of an output signal is entirely due to the charge trapped by randomly distributed Te inclusions.

IV. Polarization effect

Polarization is a function of detector's bias voltage, X-ray flux, and temperature. Therefore, polarization can be partly controlled adjusting these parameters, such as increasing bias voltage, lowering flux, and/or increasing temperature. In this work we did not change the temperature.

In some medical applications, a high flux is needed to take measurements very quickly. . CZT detectors show instability with time under bias when irradiated with a high flux, i.e. exposing a fixed area entails a gradual change in the efficiency of electron-charge collection there. . The phenomenon, generally termed the polarization effect, is characterized by a progressive degradation of energy resolutions and shifting of the peak towards the lower energy side with time after applying the bias (Fig. 5).

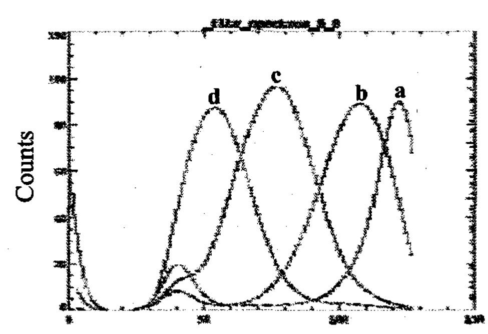

Fig. 5 Energy spectrum of a fixed area of a CZT detector: (a) Immediately t after opening the X-ray shutter, (b) after 0.5 seconds; (c) after 1 second; and (d) after 1.5 seconds. The shift of the photopeak in time is known as the polarization effect.

At the X27B beamline of NSLS the flux of the x-ray beam can be altered by changing the beam's energy. We used a monochromatic x-ray beam in the range of 8-40 keV. Fig.6 depicts the flux corresponding to the beamline.

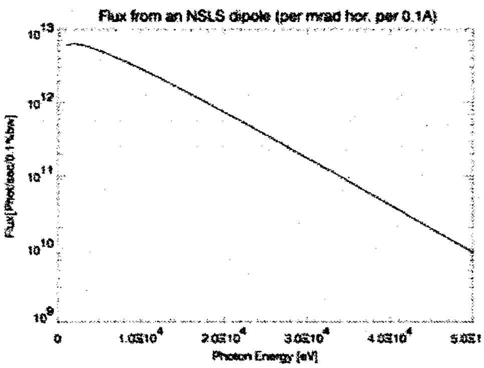

Fig. 6 Plot of the flux for an NSLS dipole versus changing energy

When measurements are needed at low flux, then a high-energy beam is employed; in contrast, in working at higher fluxes the energy of the X-ray beam is lowered. The ability to change the flux of the X-ray beam is important because we can induce polarization in certain regions and then, by lowering the flux, we can observe the X-ray map when the response of the CZT detector is stable. As discussed below, polarization behaviors differ for different regions of a CZT detector.

V. Results

Figure 7 shows one of the detectors, HX2, that we measured; it is an experimental 10mmx10mmx1mm CZT detector that we received from the crystal grower.. For the first measurement this detector was biased at 80V and an energy of 30keV was used to raster scan its entire area. .

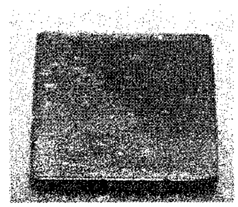

Fig. 7 Photo of the 10mm x10mm x 1mm HX2 CZT detector used in our first measurement.

Figure 8(a) shows the corresponding X-ray maps; the response is almost uniform throughout the whole area; no polarization effect was observed under these conditions. Maintaining the same bias, but increasing the flux (Fig.8b) revealed that in some regions, corresponding to the dark grey areas in the x-ray map, the detector's response had deteriorated. This is because part of the charge is trapped in these regions and then builds up, thereby lowering the external electric field. Pointing the beam at each of these regions and then closing and opening the X-ray beam shutter · energy

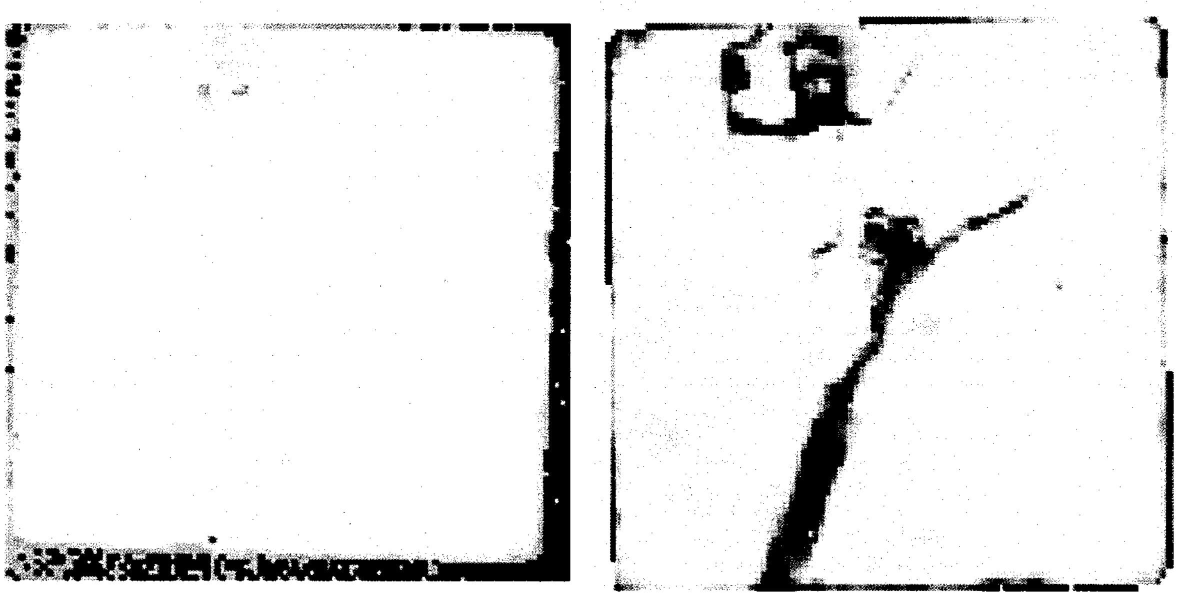

(a)

(b)

Fig. 8 Electron collection map of CZT detector HX2 when irradiated with (a) the detector's response has deteriorated.

low flux X-ray beam, and, (b) a high flux one. The latter reveals areas where

The remainder of the X-ray map in Fig 8(b) looks quite uniform. As discussed, , polarization is a function of the detector's bias voltage. When we lowered the bias voltage applied to this detector below 15V, the polarization effect becomes apparent in other regions of the detector where it previously was not observed, and furthermore, some structural defects can be observed (Fig. 9). The X-ray map in Fig. 9(a) was obtained when applying 12V and for a flux of ~10^{10}ph/sec. Fig. 9(b) shows an X-ray map obtained at 12V and for a flux 6 times higher than the previous measurement. Then, when working at lower bias (a weaker field) the pol

(a)

Fig. 9 Electron collection map of CZT detector HX2 at 12 V when irradiated with (

stronger electric field.

en irradiated with (a) l

Fig. 11 W

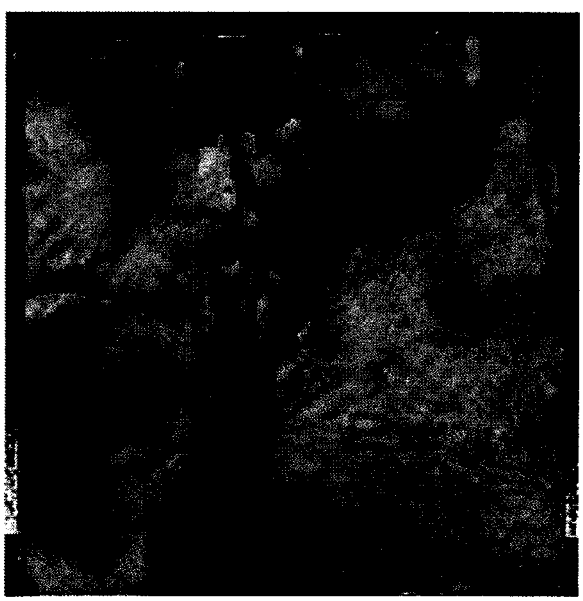

Fig. 10 Hole collection map at -170v and 31 keV

Fig. 11 WXDT image of detector HX2

hole-
do not
y low
nd for
ement
g. 10).
This is a significant result since the map contains much

information. No polarization effect is evident because the flux for this measurement is very low; Nevertheless, the hole-collection map is very similar to the electron collection map at high flux, meaning that there is a correlation between the onset of polarization and the ability to obtain a map of hole collection. Also, this map has very good spatial resolution due to the high bias applied that reduces the diffusion of the holes in the cloud. The image is very rich in what we believe to be structural defects, such as strains, subgrains, and dislocations. This observation was partially confirmed by the WXDT image of this detector shown in Fig. 11; XDT is a very powerful technique for studying structural defects in CZT crystals. The hole-collection map and the WXDT images agree quite well; nevertheless, there is a need to record the diffraction images on high resolution films to clearly see the striations observed in the map.

VI. Conclusions

Experimental CZT samples from different vendors have been studied. The polarization effect is sample-dependent; that is, samples made from the same batch of CZT materials using the same fabrication process, exhibit different polarization behaviors. A challenging task for future applications of this material is how to control the yield of low polarization detectors. Several improvements could be made to reduce the polarization effect in CZT. For the material we used, the maximum bias voltage that can be applied is limited by the leakage current. If we can reduce this, then the associated electronic noise would fall, and further, a higher bias voltage could be applied so improving the efficiency of charge collection ; concurrently, this can effectively reduce the polarization. This property is especially important when using detectors a few millimeters thick as the transit time of the free charge increases linearly with thickness for an equivalent electric field strength. Thus, the very high resistivity of CZT facilitates the improvement of the detector's performance by permitting a higher optimal bias voltage to ensure efficient charge collection, for lowering the leakage current.

Our preliminary results reveal a correlation between the onset of polarization effect and the ability to record a hole-collection map; the mechanism underlying this relationship is unclear. The structural defects observed in the map can be related to some features observed in the WXDT image, but measurements with higher resolutions are needed to reveal structural defects, such as lattice distortion and subgrain boundaries.

Acknowledgment

This work was supported by U.S. Department of Energy, Office of Nonproliferation Research and Development, NA-22. The manuscript has been authored by Brookhaven Science Associates, LLC under Contract No. DE-AC02-98CH1-886 with the U.S. Department of Energy. The United States Government retains, and the publisher, by accepting the article for publication, acknowledges, a world-wide license to publish or reproduce the published form of this manuscript, or allow others to do so, for the United States Government purposes.

References

[1] G. S. Camarda, A. E. Bolotnikov, G. A. Carini, L. Li, G. W. Wright, and R. B. James, "The Effects of Precipitates on CdZnTe Device Performance", in Proceedings of SPIE Hard X-Ray and Gamma-Ray Detector Physics VII, edited by R. B. James, L. A. Franks, and A. Burger (SPIE, Bellingham, WA, 2005), 592004-1 – 592004-7.

[2] G. A. Carini, A. E. Bolotnikov, G. S. Camarda, G. W. Wright, L. Li, and R. B. James, "Effect of Te inclusions on the performance of CdZnTe detectors", Appl. Phys. Lett. 88, p. 143515, 2006.

[3] G. S. Camarda, A. E. Bolotnikov, G. A. Carini, and R. B. James, "Effects of Tellurium Inclusions on charge collection in CZT Nuclear Radiation Detectors", in Countering Nuclear and Radiological Terrorism, edited by S. Aprkyan and D. Diamond, Springer, 2006, pp. 199-207.

[4] G. A. Carini, A. E. Bolotnikov, G. S. Camarda, R. B. James, "High-resolution x-ray mapping of CdZnTe detectors", submitted to Nucl. Instr. Meth., 2006.

[5] http://www.certif.com

[6] A. E. Bolotnikov, G. S. Camarda, G. A. Carini, Y. Cui, L. Li, and R. B. James, "Cumulative effects of Te inclusions in CdZnTe radiation detectors", submitted to Nucl. Instr. Meth. A, 2006.

[7] E. Gatti, A. Longoni, P. Rehak, and M. Sampietro, "Dynamics of electrons in drift detectors", Nucl. Instr. Meth. A253, pp. 393-399, 1987.